

# Shape-Guided Diffusion with Inside-Outside Attention

Dong Huk Park<sup>1\*</sup>  
Xihui Liu<sup>1,3†</sup>

Grace Luo<sup>1\*</sup>  
Maka Karalashvili<sup>4</sup>

Clayton Toste<sup>1</sup>  
Anna Rohrbach<sup>1</sup>

Samaneh Azadi<sup>2</sup>  
Trevor Darrell<sup>1</sup>

<sup>1</sup>UC Berkeley

<sup>2</sup>Meta AI

<sup>3</sup>The University of Hong Kong

<sup>4</sup>BMW Group

{dong.huk.park, graceluo}@berkeley.edu

\* Denotes equal contribution.

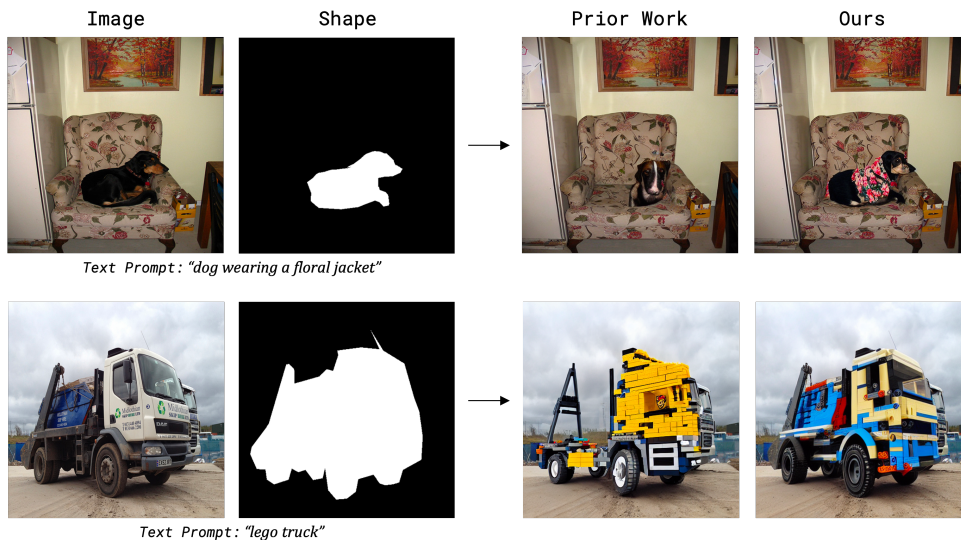


Figure 1. When a target object silhouette is available to guide the image editing process existing methods often generate objects that are poorly aligned with the given shape. We propose Shape-Guided Diffusion, a training-free method which produces shape-faithful, text-aligned, realistic objects, by using a novel Inside-Outside Attention mechanism to align the generated content with the target silhouette.

## Abstract

Shape can specify key object constraints, yet existing text-to-image diffusion models ignore this cue and synthesize objects that are incorrectly scaled, cut off, or replaced with background content. We propose a training-free method, Shape-Guided Diffusion, which uses a novel Inside-Outside Attention mechanism to constrain the cross-attention (and self-attention) maps such that prompt tokens (and pixels) referring to the inside of the shape cannot attend outside the shape, and vice versa. To demonstrate the efficacy of our method, we propose a new image editing task where the model must replace an object specified by its mask and a text prompt. We curate a new ShapePrompts benchmark based on MS-COCO and achieve

SOTA results in shape faithfulness, text alignment, and realism according to both quantitative metrics and human preferences. Our data and code will be made available at <https://shape-guided-diffusion.github.io>.

## 1. Introduction

Recent large-scale diffusion models [22, 24, 25], have significantly improved the realism of text-conditional image synthesis and its faithfulness to the input prompt. Empowering users to have further control over the synthesized images is an appealing goal. While a human can verbally describe details of a target image to be generated, there is a limit to what can be expressed via language. For instance, a specific target shape of an object may be more easily conveyed via

<sup>†</sup>This work was done when Xihui Liu was a postdoc in UC Berkeley.

a visual interface. Shape as a guidance for image editing would prevent the synthesized object from violating or disrupting the existing affordances between object entities or interactions in the scene. This capability could be beneficial for anonymization, creating targeted ads, synthetic data generation, and other applications.

Thus, we consider the task of *shape-guided editing*, where a real image and an object mask are fed to a pre-trained text-to-image diffusion model to synthesize a new object faithful to the mask’s shape and an input text prompt. Although previous works focus on the text and/or a “coarse mask” as the main tools for image editing, we show that when given a target shape, they often ignore the shape guidance by generating objects that are incorrectly scaled, cut off, or in-painted by background (see Figure 1). We observe that these models often fail at shape-guided editing because their attention maps contain spurious attentions.

We propose *Shape-Guided Diffusion*, which utilizes a novel *Inside-Outside Attention* mechanism to remove spurious attentions during image editing. This mechanism modifies the cross- and self-attention maps such that the token and pixel embeddings that refer inside the object are constrained to attend to pixels inside the shape and those that refer outside are constrained to attend outside the shape. Our method is therefore able to localize prompt-based edits within a given object mask.

We evaluate our method on MS-COCO ShapePrompts, a new benchmark we curate with MS-COCO [13] images and object masks as well as a diverse set of prompts, using the openly available Stable Diffusion codebase [24]. We achieve state-of-the-art performance in shape faithfulness, image realism, and text alignment as measured by both quantitative and qualitative evaluations, with an 11.9 point boost in mIOU and humans rating our method as more shape faithful 71% of the time.

## 2. Related Work

**Diffusion Models** Diffusion models [27] have made remarkable success in image synthesis. They define a Markov chain of diffusion steps to slowly add random noise to data and then learn to reverse the diffusion process to construct desired data samples from the noise. Variants of diffusion models include Denoising Diffusion Probabilistic Models (DDPM) [8], Denoising Diffusion Implicit Models (DDIM) [28], and score-based models [29]. Classifier guidance [4] and classifier-free guidance [9] have been investigated for conditional image synthesis with diffusion models. Diffusion models have also been adapted for conditional image synthesis [24], image inpainting [16], and image editing [12].

Cross-attention layers and their cross-modal interactions have been shown to be integral for controlling the spatial layout [7] while self-attention layers have been useful for

modeling long-range interaction between the pixels [4]. In this work, we constrain cross-attention and self-attention with object masks. The proposed Inside-Outside Attention mechanism enables shape-guided editing with diffusion models.

**Text-Guided Image Synthesis and Editing** Conditional generative models can synthesize or edit images given a text instruction. Text-guided image synthesis has been widely explored with generative models such as Generative Adversarial Networks (GAN) [33] and discrete variational autoencoders (dVAE) [23]. Recently, diffusion models [18, 23–25] have shown impressive performance on text-guided image synthesis. For text-guided image editing, StyleCLIP [20] and DiffusionCLIP [12] have shown that StyleGAN [11] and diffusion models can be guided with CLIP [21]. However, these works aim to do global rather than local edits. Blended Diffusion and GLIDE [1, 18] take both mask and text prompts as input for text-guided image editing, but they only take a rough mask and cannot precisely preserve the object shape for editing. Make-a-Scene [5] proposes an auto-regressive transformer based text-to-image generation and editing model trained via an implicit conditioning over scene tokens, derived from full segmentation maps of the scene. Although their generated images respect the object shapes, this model requires a full segmentation map during both training and inference. Conversely, our method only requires an object mask at inference time.

There are a few concurrent works in text-guided editing. Hertz *et al.* [7] propose *Cross Attention Control*, which copies cross-attention maps from a source image when generating a target image. Wu *et al.* [32] propose *CycleDiffusion*, which reuses “random seeds” from source image when generating a target image. However, our fundamental goal is different from the goals of these works. They seek to preserve the general structure between the source and target image, whereas we seek to precisely maintain the silhouette.

**Image Inpainting** Image inpainting is the task of generating missing regions of an image for object removal, image restoration, etc. Researchers have proposed dilated convolution [10], partial convolution [14], gated convolution [35], contextual attention [34], and co-modulation [37] for GAN-based image inpainting. Lugmayr *et al.* [16] recently proposed a diffusion-based [16] model for free-form image inpainting. There are two differences between our problem setup and the previous image inpainting task. First, previous image inpainting tasks use masks that often do not have semantic meaning and are free-form, whereas we use object masks. Since these masks are non-semantic, infilling the mask with background is reasonable and even encouraged. Second, previous image inpainting tasks do not use text prompts whereas ours does, enabling fine-grained control of

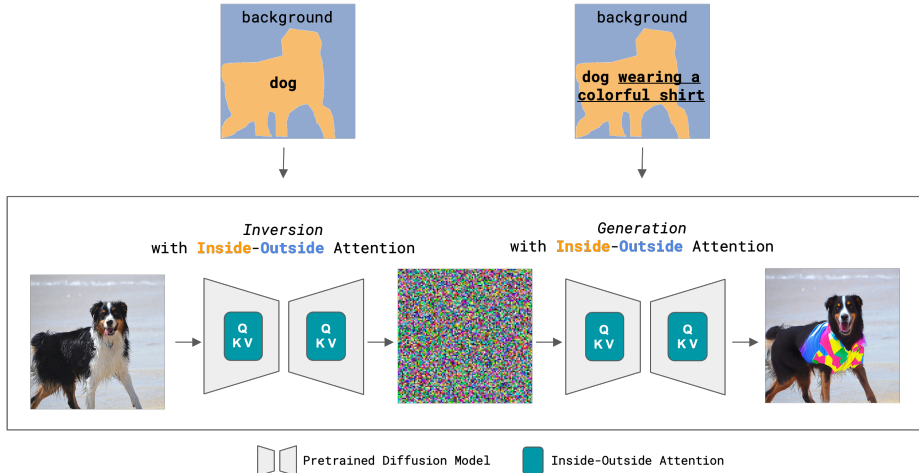


Figure 2. Shape-Guided Diffusion with Inside-Outside Attention: given two text prompts, one that describes the original object (“dog”) and one that describes the desired object (“dog wearing a colorful shirt”), we modify a pretrained diffusion model such that it respects the object’s original shape during editing. To do this, we take the object mask as an additional input and apply Inside-Outside Attention to both the inversion and generation processes to independently synthesize the object and background.

object attributes. There does exist one work, Shape-guided object inpainting [36], which also uses object masks. However, their GAN-based model requires training and cannot condition on text prompts, whereas our method is training-free and text-conditional. Recently, the authors of Latent Diffusion Models have released a variant finetuned for text-guided inpainting [17]. However, our experiments show that this training-based model still exhibits similar failure modes as these prior inpainting-based methods.

### 3. Shape-Guided Diffusion

We present Shape-Guided Diffusion, a *training-free* method that enables a pretrained text-to-image diffusion model to edit images according to the input shape masks. Our goal is to locally edit image  $x_{src}$  given an object mask  $m$  and text prompt  $\mathcal{P}_{edit}$ , generating edited image  $x_{edit}$  in which the synthesized object is not only faithful to  $\mathcal{P}_{edit}$  but also to  $m$ . We use the mechanism of Inside-Outside Attention to explicitly constrain the cross- and self-attention maps according to the object mask or inverted object mask depending on whether the token or pixel refers to the object or background. By constraining the interactions between queries and keys based on the object mask during both the inversion [4, 28] (i.e., image to noise) and generation (i.e., noise to image) processes, we are able to synthesize objects that are faithful to the original shape. The overall pipeline of our method is illustrated in Figure 2.

We build upon Stable Diffusion (SD), a Latent Diffusion Model (LDM) [24] that operates in low-resolution latent space. Note that the LDM latent space is essentially a “perceptually equivalent” downsampled version of image space, meaning we are able to apply Inside-Outside Attention in

latent space via downsampled object masks. For the rest of this paper, when we denote “pixel”, “image”, or “noise”, we are referring to these concepts in LDM latent space.

Our method is motivated by two key observations: (1) vanilla cross- and self-attention maps in diffusion models are often imperfect and contain spurious attentions and (2) if we constrain attention during the inversion process we can preserve the shape of the original object more effectively by associating specific tokens to specific object regions. In Sec. 3.1, we discuss the first key observation and how it motivates the formulation of Inside-Outside Attention. In Sec. 3.2, we elaborate on the second key observation and explain why it is important to apply Inside-Outside Attention not only during the generation, but also the inversion process.

#### 3.1. Inside-Outside Attention

LDMs contain both cross-attention layers used to produce a spatial attention map for each textual token and self-attention layers used to produce a spatial attention map for each pixel. The cross-attention layers heavily influence the image layout, and the synthesized image can have artifacts depending on the presence of spurious attentions. For example, in Figure 4, tokens that refer to one object (e.g., “horse”) may attend to other objects (e.g., “bags”) or random locations that lie outside the object region.

We postulate that prior methods often fail when given complex shapes because of these spurious attentions – attentions that seek to edit the object compete with those that seek to preserve the background because they are not well localized. Hence, we manipulate the cross-attention map such that each token is responsible for a distinct, non-

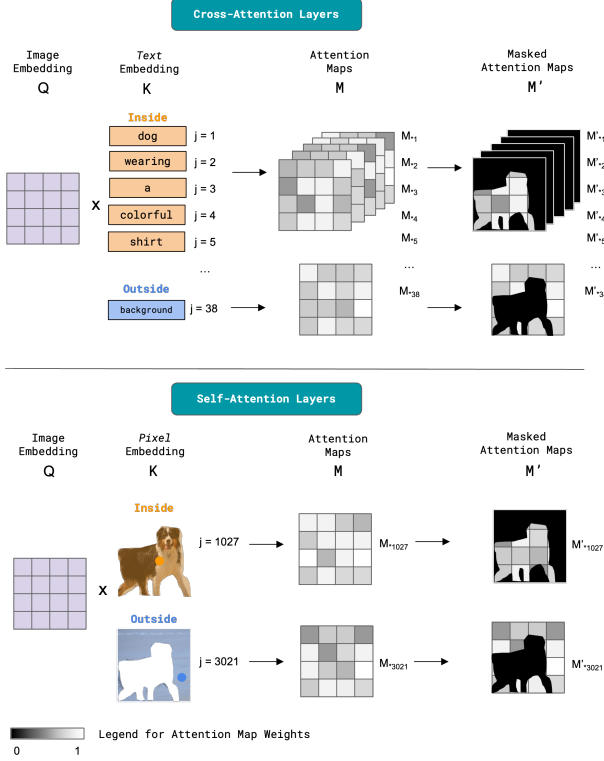


Figure 3. Inside-Outside Attention: we modify the attention maps in both the cross-attention and self-attention layers.  $j$  refers to token/pixel indices and  $M_{*j}$  denotes the attention map corresponding to the  $j$ -th index. Top: in the cross-attention layer depending on whether the text embedding refers to the inside or outside the object, we constrain the attention map  $M$  according to the object mask or the inverted object mask to produce  $M'$ . Bottom: in the self-attention layer we perform a similar operation on the inside and outside pixel embeddings.

overlapping spatial region (e.g., “horse” may only affect the horse and “background” may only affect the remaining scene). Since self-attention layers heavily influence how pixels are grouped to form coherent objects, we apply a similar manipulation to the self-attention maps to ensure that the desired object is contained within the boundaries of the input mask (i.e., only applying a cross-attention constraint centers the object within the desired region, but in some cases it may bleed into the background).

An overview for Inside-Outside Attention is given in Figure 3 and our algorithm is defined as follows (also see Alg. 1). For one forward pass, we go through all layers  $l$  of the diffusion model  $DM$  and manipulate the cross- and self-attention layers. Note that the dimension of the cross-attention maps  $M$  is  $\mathbb{R}^{H \times W \times d_\tau}$ , where  $H$  is the image height,  $W$  is the image width, and  $d_\tau$  is the number of tokens. Similarly, the dimension of the self-attention maps is  $\mathbb{R}^{H \times W \times HW}$ , where  $HW$  is the number of pixels in the flattened image. For the cross-attention layer, we determine

---

### Algorithm 1 Inside Outside Attention

---

**Input:** A diffusion model  $DM$ , a binary object mask  $m$ , a prompt  $\mathcal{P}$ .

**Output:** An edited diffusion model where the attention maps  $M$  are masked according to  $m$  and  $\mathcal{P}$  for one forward pass.

```

for all  $l \in \text{layers}(DM)$  do
  if  $\text{type}(l)$  is CrossAttention
     $J_{in} \leftarrow \{j \mid \mathcal{P}_j \text{ refers to the object}\}$ 
     $J_{out} \leftarrow \{j \mid \mathcal{P}_j \text{ refers to the background}\}$ 
  elif  $\text{type}(l)$  is SelfAttention
     $J_{in} \leftarrow \{j \mid m_j = 1\}$ 
     $J_{out} \leftarrow \{j \mid m_j = 0\}$ 
     $M_{*j_{in}} = M_{*j_{in}} \odot m \quad \forall j_{in} \in J_{in}$ 
     $M_{*j_{out}} = M_{*j_{out}} \odot (1 - m) \quad \forall j_{out} \in J_{out}$ 
  end for

```

---

the column indices  $J_{in}$  and  $J_{out}$  based on whether the token  $P_j$  refers to the object or to the background. For the self-attention layer, we determine the column indices based on whether the pixel belongs to the object  $m_j = 1$  or background  $m_j = 0$  as defined by the mask  $m$ . Finally, we mask attention map  $M_{*j_{in}}$  using  $m$  and mask attention map  $M_{*j_{out}}$  using  $1 - m$ .

### 3.2. Inversion

Denoising Diffusion Implicit Models (DDIMs) [28] are based on non-Markovian diffusion processes that give rise to a deterministic mapping from noise to images when the reverse process variance is set to 0. This gives rise to DDIM inversion, a technique where one determines the noise that produces the given real image [4]. The inverted noise is semantically meaningful, where spherical interpolation between two noises encoded from real images results in a smooth image interpolation. Hence, we initialize the generation process with the inverted noise, which often encodes shape information from the original object, allowing us to produce more natural edits on real images.

However, we observe that using DDIM inversion with a text-conditioned diffusion model can often result in a trade-off between preserving the original object shape and aligning the edited object with the prompt. We propose applying Inside-Outside Attention during DDIM inversion to mitigate this trade-off, and we are the first work to modify attention maps during DDIM inversion, to the best of our knowledge. Similar to how prior work can associate tokens to *entire images* [6, 31], with Inside-Outside Attention we can associate tokens to *specific object regions*. This means that if we include tokens used to describe the original object in the inversion process (e.g. “dog”) into the new prompt used in the generation process (e.g. “dog wearing a colorful shirt”), we carry a lot of shape information into the edited

image through the shared tokens (e.g. “dog”) as seen in Figure 2. Without the Inside-Outside Attention, these similarities would be far less pronounced because the shape information would be spread across other prompt tokens that do not necessarily pertain to the object region.

### 3.3. Shape-Guided Diffusion Pipeline

We leverage these two key insights in our Shape-Guided Diffusion method by applying Inside-Outside Attention during both the inversion and generation process. An overview of our method can be found in Figure 2 and the algorithm can be defined as follows (also see Alg. 2). We first activate Inside-Outside Attention and run DDIM inversion on the conditional diffusion model driven by the prompt  $\mathcal{P}_{src}$  (e.g. “dog”). We set our initial noise  $z_T$  to the inverted noise  $\bar{z}_T$ . For each diffusion step, we activate Inside-Outside attention for both the conditional and unconditional diffusion models using both mask  $m$  and  $\mathcal{P}_{edit}$  (e.g. “dog wearing a colorful shirt”). We mix the predictions of both models following classifier-free guidance [8]. Note that we apply the guidance to the conditional prediction  $z_{cond}$  similar to Ho *et al.* [8] rather than the unconditional prediction  $z_{uncond}$  as popularized by the LDM implementation since we use the conditional model during inversion and empirically find that this design choice leads to higher text alignment without a loss in other metrics. Finally, we copy back the noised version of the real image found during the inversion process  $\bar{z}_{t-1}$  as the background to form the edited image prediction  $z_{t-1}$ . This ensures that the edited image  $x_{edit}$  and the original image  $x_{src}$  only differ within the mask region  $m$ .

---

#### Algorithm 2 Shape-Guided Diffusion

---

**Input:** A diffusion model  $DM$  with autoencoder  $\mathcal{E}$ , real image  $x_{src}$ , a binary object mask  $m$ , a source prompt  $\mathcal{P}_{src}$ , an edit prompt  $\mathcal{P}_{edit}$ .

**Hyperparameters:** Classifier-free guidance scale  $w_g$ .

**Output:** An edited image  $x_{edit}$  that differs from  $x_{src}$  only within the mask region  $m$ .

```

SetInsideOutsideAttention( $DM, \mathcal{P}_{src}, m$ )
 $[\bar{z}_0, \dots, \bar{z}_T] \sim \text{DDIMInversion}(z|\mathcal{E}(x_{src}), \mathcal{P}_{src}, DM)$ 
 $z_T \leftarrow \bar{z}_T$ 
for all  $t$  from  $T$  to  $0$  do
  SetInsideOutsideAttention( $DM, \mathcal{P}_{edit}, m$ )
   $z_{cond} \leftarrow DM(z_t, \mathcal{P}_{edit})$ 
   $z_{uncond} \leftarrow DM(z_t, \emptyset)$ 
   $z_{t-1} \leftarrow z_{cond} + w_g * (z_{uncond} - z_{cond})$ 
   $z_{t-1} \leftarrow z_{t-1} \odot m + \bar{z}_{t-1} \odot (1 - m)$ 
end for

```

---

## 4. MS-COCO ShapePrompts

**Benchmark** We evaluate our approach on MS-COCO images [13] since it contains images of common objects in context paired with object masks. We filter for object masks with an area between [2%, 50%] of the image, as we would like to edit objects that are not too small (LDMs [24] have relatively coarse resolution scales) and not too large (shape-guidance for masks that span the entire or majority of the image reduces to full image synthesis). Our test set derived from MS-COCO val 2017 contains 1,149 object masks spanning 10 categories: “bear”, “bird”, “cat”, “dog”, “elephant”, “horse”, “sandwich”, “boat”, “kite”, and “truck”. We select these categories spanning various animal, vehicle, food, and sports types because they encompass a wide variety of possible poses, deformations, and textures. We create a validation set with 1,000 object masks in the same fashion derived from MS-COCO train 2017.

For each of the 10 categories, we design a few prompts intended to produce images that are visually striking and distinct from real MS-COCO images. Most of the prompts add clothing or accessories (e.g. “floral shirt” or “sunglasses”), manipulate color (e.g. “iridescent”, “with spray paint graffiti”), switch material (“lego”, “paper”), or specify rare subcategories (“spotted leopard cat”, “tortilla wrapped sandwich”). These prompts were inspired by examples from prior work [1, 7] and a search engine with paired prompts and synthetic images from Stable Diffusion [26]. More information about the prompts can be found in the Supplemental.

**Metrics** Since we aim to synthesize an image faithful to the input shape, we use mean Intersection over Union (mIoU) as a metric. Specifically, we compute the proportion of pixels within the masked region synthesized according to the desired object class versus other classes, as determined by a segmentation model [3] pretrained on COCO-Stuff [2]. See Supplemental for more details. We also report FID scores as a metric for image realism, which measures the similarity of the distributions of real and synthetic images using the features of an Inception network [19, 30]. Finally, we report CLIP [21] scores as a metric for image-text alignment, which measures the similarity of the text prompt and synthetic image using the features of a large pretrained image-text model.

## 5. Experiments

We run quantitative and qualitative evaluations on the shape-guided editing task where the model must replace an object given a (real image, object mask, text prompt) triplet from MS-COCO ShapePrompts. We report metrics for shape faithfulness, image realism, and text alignment (Sec. 4).

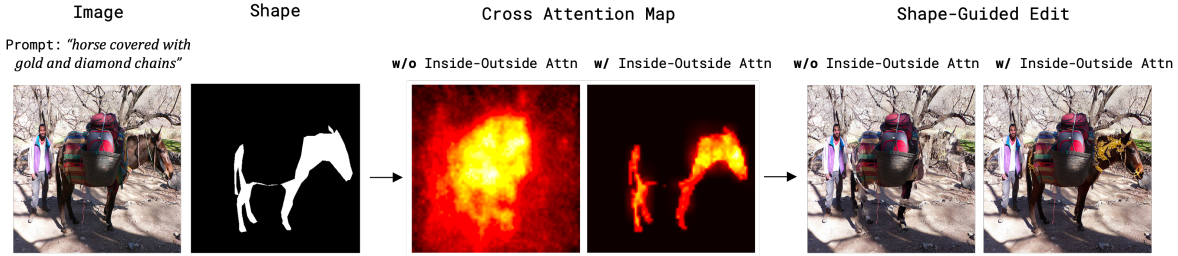


Figure 4. Visualization of cross-attention maps without (w/o) and with (w/) Inside-Outside Attention. Given a real image and prompt (“horse covered with gold and diamond chains”), we visualize the cross attention maps averaged over all layers and timesteps for the token “horse” during generation. Note how without Inside-Outside Attention the token not only attends to the horse but also the person and the bags, but with the mechanism the token’s attention is localized to the correct region.



Figure 5. Comparison to prior work. We compare our results with Blended Diffusion and SD-Inpaint. Both baselines fail to be consistent with either the shape masks or the text prompts, whereas our method is able to generate realistic edits that are faithful to the prompt while preserving the original shape.

**Blended Diffusion** We compare against Blended Diffusion [1], which demonstrates prompt and mask driven editing on Guided Diffusion, an unconditional diffusion model [4]. The method composites noise predictions with the real image’s background to abide by the spatial constraint of the input mask and uses CLIP for text-based classifier guidance to fill the mask according to the prompt.

**SD-Inpaint** We also compare against a variant of Stable Diffusion specifically *finetuned* for text-and-mask conditioned inpainting [17]. The model adds an extra channel to the UNet architecture to accept masks as input.

**Ours** For our Shape-Guided Diffusion model we use Stable Diffusion as a backbone. To do this, we apply the Inside-

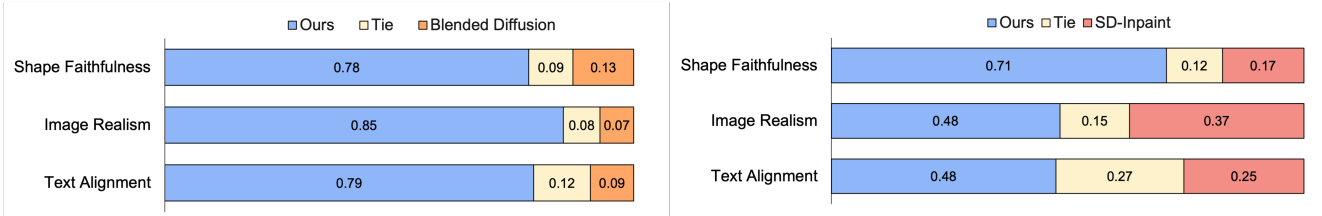


Figure 6. Qualitative comparison to baselines on MS-COCO ShapePrompts (100-sample subset of test set). We display the percentage of samples where humans preferred images synthesized by Ours vs. Blended Diffusion (left) and Ours vs. SD-Inpaint (right) along various metrics, where the method used to synthesize the image was anonymized and in randomized order in both evaluations.

Approach	mIOU ( $\uparrow$ )	FID ( $\downarrow$ )	CLIP ( $\uparrow$ )
Real Images	76.3	-	0.15
Blended Diffusion	41.8	46.2	0.20
SD-Inpaint	51.7	43.7	0.19
Ours	<b>63.6</b>	<b>40.2</b>	<b>0.21</b>

Table 1. Quantitative comparison to the baselines on MS-COCO ShapePrompts (test set).

Outside Attention mechanism in a *training-free* fashion.<sup>1</sup>

**Experimental Setup** For both Blended Diffusion and SD-Inpaint we use the default hyperparameters provided by their respective repositories. For sampling we use a standard DDIM scheduler for 50 inversion and generation steps. When using Inside-Outside Attention on cross-attention layers, we evenly divide the maximum number of text tokens excluding the `<bos>` token, resulting in 38 “inside” tokens and 38 “outside” tokens. The attentions for `<bos>` token are simply zeroed out.

## 5.1. Comparison to Prior Work

In Figure 5, we depict real images (first row) and edits made by Blended Diffusion (second row), SD-Inpaint (third row), and Ours (fourth row). Prior works demonstrate a variety of failure modes in shape-guided editing, where an object may be transformed into a new shape, removed completely, severely downscaled, or rendered without respecting the prompt. On the other hand, our method is able to simultaneously respect the shape and the prompt without a compromise in image realism. These same trends can be observed in our quantitative evaluation displayed in Table 1, where our method outperforms the baselines in all metrics, with an improvement of 11.9 in mIOU, 3.5 in FID, and 1.0 in CLIP score as measured over more than one thousand samples from MS-COCO ShapePrompts test set.

We also conduct a qualitative evaluation to confirm that our observations and quantitative evaluation corre-

<sup>1</sup>We use the weights provided by <https://huggingface.co/runwayml/stable-diffusion-inpainting> and <https://huggingface.co/runwayml/stable-diffusion-v1-5> for SD-Inpaint and Ours respectively.

late with human judgments. We created two evaluations with five participants each, one that compared Ours vs. Blended Diffusion and another that compared Ours vs. SD-Inpaint. Each evaluation contained 100 samples from the MS-COCO ShapePrompts test set, each composed of a synthetic image from each method *in a randomized order* with the original image and shape for reference. Five people were asked to rate each sample, where they compared the two synthetic images and selected the one that scored the best along shape faithfulness, image realism, and text alignment. They were also given the option to select a “Tie” if both images were comparable along the metric. Please see Supplemental for further details.

In Figure 6, we report the results of these two evaluations. For shape faithfulness, our method significantly outperforms both Blended Diffusion and SD-Inpaint, as seen in the first row where humans preferred our method 78% and 71% of the time, respectively. In image realism and text alignment, our method beats Blended Diffusion by a large margin where humans prefer our method 79 – 85% of the time. Most notably, in image realism and text alignment our method is preferred or tied with SD-Inpaint majority of the time, indicating that our method is not only able to improve shape faithfulness without compromising other metrics, but it is also able to *improve* quality in other metrics at the same time. Even more, while SD-Inpaint is a strong baseline *fine-tuned* to produce realistic objects given a mask, humans still prefer our *training-free* method across the board.

## 5.2. Ablations

We report an ablation study in Table 2. (1) uses a standard guidance scale of 7.5 and copies the background of the real image onto the prediction at each timestep as done in Blended Diffusion [1], (2) uses DDIM inverted noise during the generation process, (3) re-weights cross-attention maps based on the change between  $\mathcal{P}_{src}$  and  $\mathcal{P}_{edit}$  as done in Cross Attention Control [7]<sup>2</sup>, (4) applies Inside-Outside Attention only to the cross-attention layers (Token Inside-Outside Attn), (5) applies Inside-Outside Attention with

<sup>2</sup>When re-weighting, we use a constant scalar upweighting of 2.5 as determined by hyperparameter sweeps in early experiments.

Approach	Guidance Scale	mIOU ( $\uparrow$ )	FID ( $\downarrow$ )	CLIP ( $\uparrow$ )
Real Images	N/A	78.6	-	0.16
(1) SD	7.5	52.5	46.2	0.21
(2) SD + DDIM Inv	7.5	61.2	42.8	0.21
(3) SD + DDIM Inv + Re-Weight	3.5	59.6	40.6	0.21
(4) SD + DDIM Inv + Re-Weight + Token Inside-Outside Attn	3.5	62.9	40.6	0.21
(5) SD + DDIM Inv + Re-Weight + Soft Inside-Outside Attn	3.5	66.2	40.2	0.21
(6) SD + DDIM Inv + Re-Weight + Hard Inside-Outside Attn (Ours)	3.5	<b>67.6</b>	<b>39.0</b>	0.21

Table 2. Ablations on MS-COCO ShapePrompts (validation set).



Figure 7. Inter-class and Outside edits. Our method is not only capable of doing intra-class edits, but also inter-class edits while preserving the object shape. Additionally, by augmenting the outside tokens—namely the “background” token—with additional descriptions, our method is able to edit regions outside of the object mask.

a hard mask for the cross-attention and soft mask for the self-attention layers (Soft Inside-Outside Attn), and (6) applies Inside-Outside Attention with a hard mask for both the cross- and self-attention layers (Hard Inside-Outside Attn), the design used in our final method. Comparing (1) and (2), we show that using DDIM inverted noise helps in both mIOU and FID. For (3), we empirically find that higher guidance scale, when used in combination with DDIM inversion, makes the model rely less on the the inverted noise, resulting in less realistic editing. However, we find that simply lowering the guidance scale leads to degradation in text faithfulness. Using cross-attention re-weighting mitigates this issue and allows us to achieve better image realism with similar performance in shape and text faithfulness. In (4), when we apply the Inside-Outside Attention mechanism only to the cross-attention layers we observe a small boost in mIOU with the same FID score, and when we apply it to both the cross- and self-attention layers in (5) we observe a more significant boost of 6.6 points in mIOU and 0.4 points in FID from (3). Comparing (5) and (6) we find that using a hard mask for Inside-Outside Attention performs better than using a soft mask, as seen by the further boost of 1.4 points in mIOU and 1.2 points in FID. Our final method that combines DDIM inversion, re-weighting, and hard Inside-Outside Attention achieves the best performance in mIOU and FID with scores of 67.6 and 39.0 respectively without a degradation in CLIP score.

### 5.3. Additional Editing Results

In [Figure 7](#), we demonstrate additional capabilities of our method, including inter-class and background edits. On the

left side, we demonstrate how an image of a cow can both be edited to wear “gold and diamond chains” and to transform into a “sheep” (a different class) while preserving the original shape. On the right side, we demonstrate how our method is not only able to associate object tokens but also background tokens with image regions, as seen by how we are able to transform the background to a background “at sunset” and “in front of the Eiffel Tower in Paris.” Note how our edits maintain structures in the real image; the cabinet at the top is transformed into a landmass in the edited images and the sink is transformed into ripples or tiling in the edited images, all while preserving the original cat.

## 6. Conclusion

In this work, we proposed shape as a new editing interface for diffusion models. We have shown that existing text-to-image synthesis models fail to respect shape, which is likely caused by spurious attentions. In this work, we propose Shape-Guided Diffusion, a training-free method that uses a novel Inside-Outside Attention mechanism during both the inversion and generation process. To evaluate our method, we curate the MS-COCO ShapePrompts dataset. In this benchmark, the goal is to edit an object in a real image according to an input mask and a text prompt. We show that our method significantly outperforms the baselines in shape faithfulness with additional improvements in realism and text alignment.

**Acknowledgements.** This work was supported in part by DoD including DARPA’s SemaFor, PTG and/or LwLL programs, as well as BAIR’s industrial alliance programs.

## References

- [1] Omri Avrahami, Dani Lischinski, and Ohad Fried. Blended diffusion for text-driven editing of natural images. In *CVPR*, 2022. 2, 5, 6, 7
- [2] Holger Caesar, Jasper Uijlings, and Vittorio Ferrari. Cocosuff: Thing and stuff classes in context. In *CVPR*, 2018. 5
- [3] Bowen Cheng, Alexander G. Schwing, and Alexander Kirillov. Per-pixel classification is not all you need for semantic segmentation. In *NeurIPS*, 2021. 5, 11, 13, 19
- [4] Prafulla Dhariwal and Alexander Nichol. Diffusion models beat gans on image synthesis. In *NeurIPS*, 2021. 2, 3, 4, 6
- [5] Oran Gafni, Adam Polyak, Oron Ashual, Shelly Sheynin, Devi Parikh, and Yaniv Taigman. Make-a-scene: Scene-based text-to-image generation with human priors. *arXiv preprint arXiv:2203.13131*, 2022. 2
- [6] Rinon Gal, Yuval Alaluf, Yuval Atzmon, Or Patashnik, Amit H Bermano, Gal Chechik, and Daniel Cohen-Or. An image is worth one word: Personalizing text-to-image generation using textual inversion. *arXiv preprint arXiv:2208.01618*, 2022. 4
- [7] Amir Hertz, Ron Mokady, Jay Tenenbaum, Kfir Aberman, Yael Pritch, and Daniel Cohen-Or. Prompt-to-prompt image editing with cross attention control. *arXiv preprint arXiv:2208.01626*, 2022. 2, 5, 7
- [8] Jonathan Ho, Ajay Jain, and Pieter Abbeel. Denoising diffusion probabilistic models. In *NeurIPS*, 2020. 2, 5
- [9] Jonathan Ho and Tim Salimans. Classifier-free diffusion guidance. *arXiv preprint arXiv:2207.12598*, 2022. 2
- [10] Satoshi Iizuka, Edgar Simo-Serra, and Hiroshi Ishikawa. Globally and locally consistent image completion. *ACM Transactions on Graphics (ToG)*, 36(4):1–14, 2017. 2
- [11] Tero Karras, Samuli Laine, and Timo Aila. A style-based generator architecture for generative adversarial networks. In *CVPR*, 2019. 2
- [12] Gwanghyun Kim, Taesung Kwon, and Jong Chul Ye. Diffusionclip: Text-guided diffusion models for robust image manipulation. In *CVPR*, 2022. 2
- [13] Tsung-Yi Lin, Michael Maire, Serge Belongie, Lubomir Bourdev, Ross Girshick, James Hays, Pietro Perona, Deva Ramanan, C. Lawrence Zitnick, and Piotr Dollár. Microsoft coco: Common objects in context. In *ECCV*, 2014. 2, 5
- [14] Guilin Liu, Fitsum A Reda, Kevin J Shih, Ting-Chun Wang, Andrew Tao, and Bryan Catanzaro. Image inpainting for irregular holes using partial convolutions. In *ECCV*, 2018. 2
- [15] Timo Lüddecke and Alexander Ecker. Image segmentation using text and image prompts. In *Proceedings of the IEEE/CVF Conference on Computer Vision and Pattern Recognition (CVPR)*, pages 7086–7096, June 2022. 11
- [16] Andreas Lugmayr, Martin Danelljan, Andres Romero, Fisher Yu, Radu Timofte, and Luc Van Gool. Repaint: Inpainting using denoising diffusion probabilistic models. In *CVPR*, 2022. 2
- [17] Runway ML. Stable diffusion inpainting. <https://huggingface.co/runwayml/stable-diffusion-inpainting>, 2022. 3, 6
- [18] Alex Nichol, Prafulla Dhariwal, Aditya Ramesh, Pranav Shyam, Pamela Mishkin, Bob McGrew, Ilya Sutskever, and Mark Chen. Glide: Towards photorealistic image generation and editing with text-guided diffusion models. In *ICML*, 2022. 2
- [19] Gaurav Parmar, Richard Zhang, and Jun-Yan Zhu. On aliased resizing and surprising subtleties in gan evaluation. In *CVPR*, 2022. 5
- [20] Or Patashnik, Zongze Wu, Eli Shechtman, Daniel Cohen-Or, and Dani Lischinski. Styleclip: Text-driven manipulation of stylegan imagery. In *ICCV*, 2021. 2
- [21] Alec Radford, Jong Wook Kim, Chris Hallacy, Aditya Ramesh, Gabriel Goh, Sandhini Agarwal, Girish Sastry, Amanda Askell, Pamela Mishkin, Jack Clark, et al. Learning transferable visual models from natural language supervision. In *ICML*, 2021. 2, 5, 11
- [22] Aditya Ramesh, Prafulla Dhariwal, Alex Nichol, Casey Chu, and Mark Chen. Hierarchical text-conditional image generation with clip latents. *arXiv preprint arXiv:2204.06125*, 2022. 1
- [23] Aditya Ramesh, Mikhail Pavlov, Gabriel Goh, Scott Gray, Chelsea Voss, Alec Radford, Mark Chen, and Ilya Sutskever. Zero-shot text-to-image generation. In *ICML*, 2021. 2
- [24] Robin Rombach, Andreas Blattmann, Dominik Lorenz, Patrick Esser, and Björn Ommer. High-resolution image synthesis with latent diffusion models. In *CVPR*, 2022. 1, 2, 3, 5
- [25] Chitwan Saharia, William Chan, Saurabh Saxena, Lala Li, Jay Whang, Emily Denton, Seyed Kamyar Seyed Ghasemipour, Burcu Karagol Ayan, S Sara Mahdavi, Rapha Gontijo Lopes, et al. Photorealistic text-to-image diffusion models with deep language understanding. *arXiv preprint arXiv:2205.11487*, 2022. 1, 2
- [26] Sharif Shameem. Lexica. <https://lexica.art/>, 2022. 5
- [27] Jascha Sohl-Dickstein, Eric Weiss, Niru Maheswaranathan, and Surya Ganguli. Deep unsupervised learning using nonequilibrium thermodynamics. In *ICML*, 2015. 2
- [28] Jiaming Song, Chenlin Meng, and Stefano Ermon. Denoising diffusion implicit models. In *ICLR*, 2021. 2, 3, 4
- [29] Yang Song, Jascha Sohl-Dickstein, Diederik P Kingma, Abhishek Kumar, Stefano Ermon, and Ben Poole. Score-based generative modeling through stochastic differential equations. In *ICLR*, 2021. 2
- [30] Christian Szegedy, Vincent Vanhoucke, Sergey Ioffe, Jon Shlens, and Zbigniew Wojna. Rethinking the inception architecture for computer vision. In *Proceedings of the IEEE conference on computer vision and pattern recognition*, pages 2818–2826, 2016. 5
- [31] Dani Valevski, Matan Kalman, Yossi Matias, and Yaniv Leviathan. Unitune: Text-driven image editing by fine tuning an image generation model on a single image. *arXiv preprint arXiv:2210.09477*, 2022. 4
- [32] Chen Henry Wu and Fernando De la Torre. Unifying diffusion models’ latent space, with applications to cyclediffusion and guidance. *arXiv preprint arXiv:2210.05559*, 2022. 2

- [33] Tao Xu, Pengchuan Zhang, Qiuyuan Huang, Han Zhang, Zhe Gan, Xiaolei Huang, and Xiaodong He. Attngan: Fine-grained text to image generation with attentional generative adversarial networks. *CVPR*, 2018. 2
- [34] Jiahui Yu, Zhe Lin, Jimei Yang, Xiaohui Shen, Xin Lu, and Thomas S Huang. Generative image inpainting with contextual attention. In *CVPR*, 2018. 2
- [35] Jiahui Yu, Zhe Lin, Jimei Yang, Xiaohui Shen, Xin Lu, and Thomas S Huang. Free-form image inpainting with gated convolution. In *ICCV*, 2019. 2
- [36] Yu Zeng, Zhe Lin, and Vishal M Patel. Shape-guided object inpainting. *arXiv preprint arXiv:2204.07845*, 2022. 3
- [37] Shengyu Zhao, Jonathan Cui, Yilun Sheng, Yue Dong, Xiao Liang, Eric I Chang, and Yan Xu. Large scale image completion via co-modulated generative adversarial networks. 2021. 2

## Supplementary Material

In Section A we discuss details regarding the MS-COCO ShapePrompts benchmark, in Section B we discuss details regarding our qualitative evaluation, in Section C we show success and failure cases, and in Section D we show additional editing settings our method is capable of.

### A. MS-COCO ShapePrompts Details

**Prompts** For our MS-COCO ShapePrompts benchmark we design a set of prompts where it is possible to simultaneously synthesize an object that is shape faithful and text aligned (as opposed to prompts entangled with shape, i.e., transforming “chihuahua dog” to “poodle dog” while respecting shape is difficult because poodles are characterized by floppy ears and fluffy fur). While our method is able to perform inter-class edits as seen in Figure 7, we focus our experiments on intra-class edits which make more sense given the shape constraint (e.g. some hyper-specific shapes like the silhouette of an elephant only make sense when edits are done within the object class). For this reason we design prompts for each object class as seen below in Figure 8.

```
prompts = {
  "bear": [
    "stuffed {}",
    "{} wearing sunglasses"
  ],
  "bird": [
    "{} with blue and yellow feathers",
    "{} with iridescent feathers"
  ],
  "cat": [
    "spotted leopard {}",
    "{} wearing a yellow and black tie"
  ],
  "dog": [
    "{} wearing a floral jacket",
    "{} wearing a colorful shirt"
  ],
  "elephant": [
    "{} wearing christmas decorations",
    "holi festival {}"
  ],
  "horse": [
    "futuristic biomechanical robotic {} with synthetic body parts showing",
    "{} covered with gold and diamond chains"
  ],
  "sandwich": [
    "tortilla wrapped {}",
    "{} with peanut butter and jelly filling"
  ],
  "boat": [
    "inflatable {}",
    "{} made of candies"
  ],
  "kite": [
    "origami {} made of paper",
    "glitter {}"
  ],
  "truck": [
    "lego {}",
    "{} with spray paint graffiti"
  ],
}
```

Figure 8. Prompts from the MS-COCO ShapePrompts benchmark.

**Shape Faithfulness Metric** To measure shape faithfulness we use the pretrained segmentation model MaskFormer [3]. We demonstrate that the model makes meaningful predictions on synthetic images in Figure 9. Even more, the model’s predictions are reasonably robust to out-of-

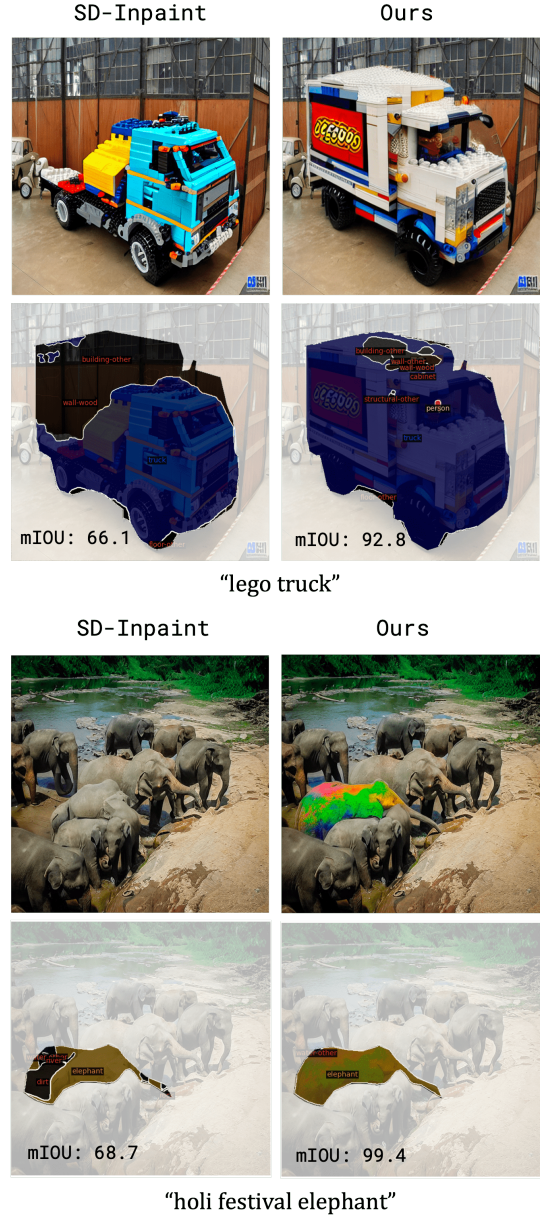


Figure 9. Synthetic images and their corresponding predicted segmentation and mIOU. Note how these out-of-distribution variants of the object class, such as a truck made of legos or elephant painted with dyes, are still segmented correctly.

distribution variants of the object class, such as “lego truck.” We also tried the referring expression segmentation model ClipSeg [15], which advertises open-vocabulary segmentation abilities with CLIP [21] as the visual backbone. However, in early experiments we found that ClipSeg had lower recall and worse coverage when segmenting the synthesized object compared with MaskFormer [3].

We use our pretrained segmentation model to compute mean intersection over union (mIOU). We compute mIOU on a per-sample basis (i.e., we average the IOU of each object regardless of size) as opposed to a per-pixel basis (which is typically used in semantic segmentation works) since it is equally important to synthesize both small and large objects in a shape-faithful fashion. We set all pixels outside the mask to a null prediction to compute mIOU only within the edited mask region.

## B. Qualitative Evaluation Details

Our qualitative evaluation included 10 total participants divided across two evaluations. We asked each participant to rate 100 samples, where they were told that they would be “rating AI-edited images, where the goal is to edit one object according to a text prompt while maintaining its shape.” Each sample was formatted as pictured in Figure 10, in the grid the first column (“Original”) corresponds to the original image, the second column (“A”) corresponds to an edited image, and the third column (“B”) corresponds to another edited image. To help participants judge faithfulness in addition to the first row (“Full Image”) we also provide the second row (“Masked Object”) which masks the full image according to the shape of the original object. Along the metrics of shape faithfulness, text alignment, and image realism we asked participants to rate whether synthetic image A or B performed better, or whether they “Tie.” We define the metrics using the following instructions:

### 1. Shape

*Definition:* The edited object matches the scale and silhouette of the original object, and it is not cut off, zoomed out, or zoomed in. If both edited objects are similar in shape faithfulness, you may tie-break by judging the pose.

*Heuristic:* The edited object fills the masked version of the image in the “Masked Object” row.

### 2. Text

*Definition:* The edited object matches the text prompt.

*Heuristic:* The edited object matches what you were imagining given the text prompt.

### 3. Realism

*Definition:* The edited image looks realistic and lacks visual artifacts or logical flaws.

*Heuristic:* If you saw it on the internet you would believe the image is a real photograph / created by a human artist.

We also gave participants the option to mark whether one of the synthetic image makes no substantial edit to the original object (i.e. the image copies and recolors the same object), which would be unfairly marked as having better shape faithfulness and image realism at the cost of text alignment under our evaluation standard. We removed these marked samples from our final comparison, resulting in the removal of 25 out of 1000 total samples (from 10 participants rating 100 images each) across both evaluations.

## C. Success / Failure Cases

**Success Cases.** In Figure 11 we show our synthesized images for each prompt in the MS-COCO ShapePrompts

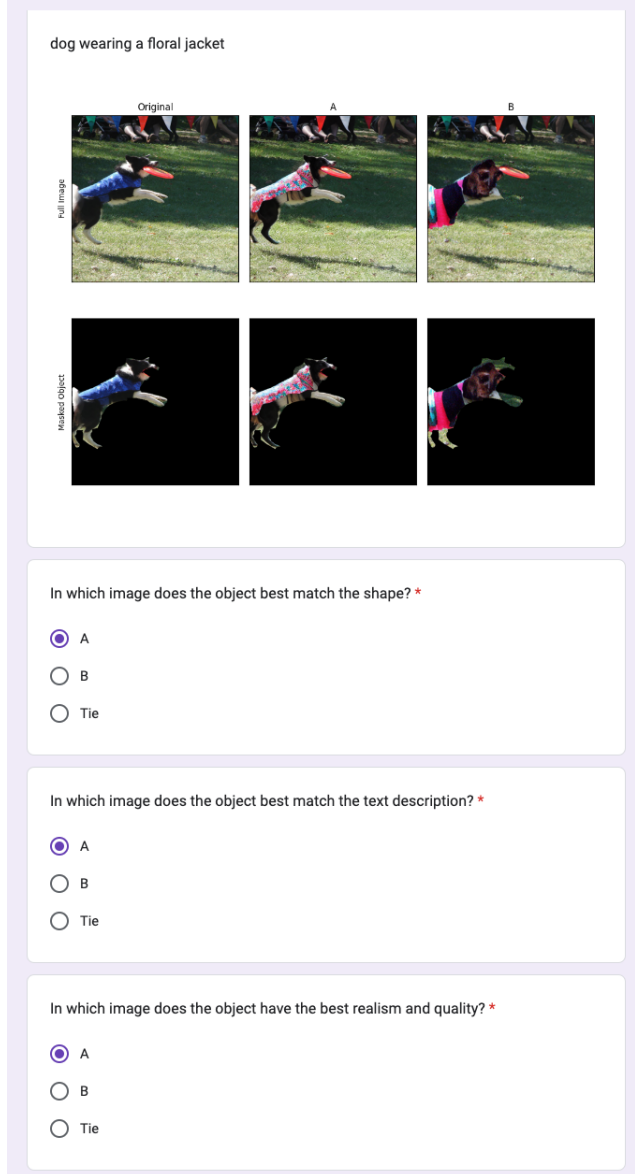


Figure 10. Screenshot of our qualitative evaluation. Participants were asked to compare images synthesized by our method versus a baseline in random order and rate (1) shape faithfulness, (2) text alignment, (3) image realism.

benchmark. We demonstrate that our method is able to handle partially occluded masks and maintain relationships between the object and background, as seen in the case of the “inflatable boat” where the edit maintains the position of the man and dog on that boat. We demonstrate that our method is able to add accessories while simultaneously respecting the input shape, as seen by the “elephant wearing christmas decorations” where an ear is converted to a santa hat. Finally, our method is seamlessly able to edit material

(“lego truck”, “boat made of candies”, “origami kite made of paper”) and color (“truck with spray paint graffiti”, “bird with iridescent feathers”, “holi festival elephant”).

**Failure Cases.** We also show failure cases of our method in [Figure 12](#). Sometimes the shape is inherently difficult, such as the case with (a) uncommon pose (i.e., our method repositions an elephant sitting on its hind legs to standing), (b) uncommon perspective (i.e., our method transforms a close-up of a dog’s eyes to a dog’s entire face and converts its hair into fabric to abide by the “floral jacket” in the prompt), or (c) multi-part mask inputs (i.e., our method only edits the front half of the truck into a lego material). Since we use DDIM inversion (d) ghosting can occur where remnants of the original object (e.g. a mouth or ear) can appear in the synthesized object. Since we localize the attention maps (e) global context can be ignored (i.e., our method edits a colorful dog into a black-and-white photo or creates artifacts at the boundary between a dog’s legs and water). Finally, our method may produce strange (f) accessory placement (i.e., our method places a bowtie on the cat’s arm because its neck is not visible in the original image).

## D. Additional Editing Settings

**Inter-Class and Background Edits.** Building on our discussion in [Section 5.3](#), we show additional examples of inter-class edits in [Figure 13](#), including converting from cat to dog, dog to cat, or sheep to cow. We also show additional examples of background edits in [Figure 14](#), including transforming the background to different locations, seasons, or times of day for various objects.

**Simultaneous Inside-Outside Edits.** In [Figure 15](#) we demonstrate examples of *simultaneous* inside-outside editing. Since our method allows us to localize and separate the editing of the object and background, we can simultaneously edit both with two different prompts. This property allows us to maintain the relation of the object with the scene (e.g., the silhouette and exact position of the horse grazing on grass) and significantly modify both objects (e.g., converting the horse to a “futuristic biomechanical robot” and the background to the “Metropolitan Museum of Art.”

**Inferred Segmentation Mask Edits.** Although in our experiments we use the instance-level masks provided by MSCOCO, we also demonstrate that our method also works on *automatically inferred* masks. We run MaskFormer [3] to segment the image and identify regions that correspond to a specific object class to create a binary mask. Note that since we use a semantic segmentation model there is no marking of individual instances, so our method may be asked to edit multiple objects given one text prompt. As seen in

[Figure 16](#), our method is able to handle this setting with multiple instances, whether that means synthesizing given the (a) reflection of one object, (b) the existence of multiple disjoint objects, or (c) the existence of multiple overlapping objects. In cases with (d) imperfect masks that bleed onto other object classes, our method is able to appropriately edit the object class of interest without negatively impacting the realism of other object classes. Finally, for some images the segmentation model produces (e) standard clean masks containing single objects, which our method is able to handle. As such, we demonstrate that our method is reasonably robust to a variety of masks. In a real world setting, this means that an off-the-shelf segmentation model can be used to infer the shape, allowing the user to only input an image and prompt referencing the object they would like to edit.

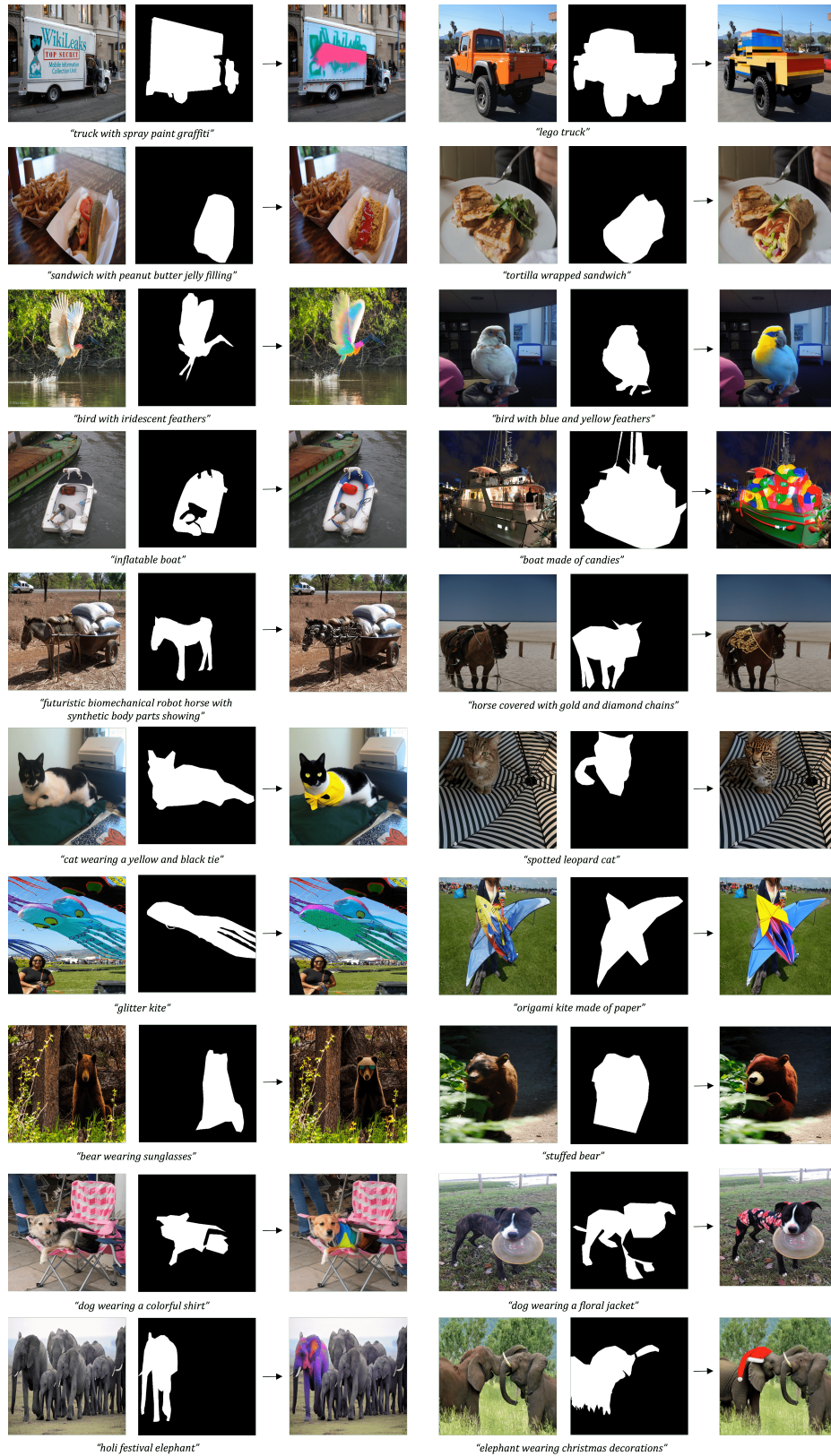


Figure 11. Examples of success cases from our method that demonstrate its ability to handle partially occluded masks, add accessories, transform materials, or recolor objects.

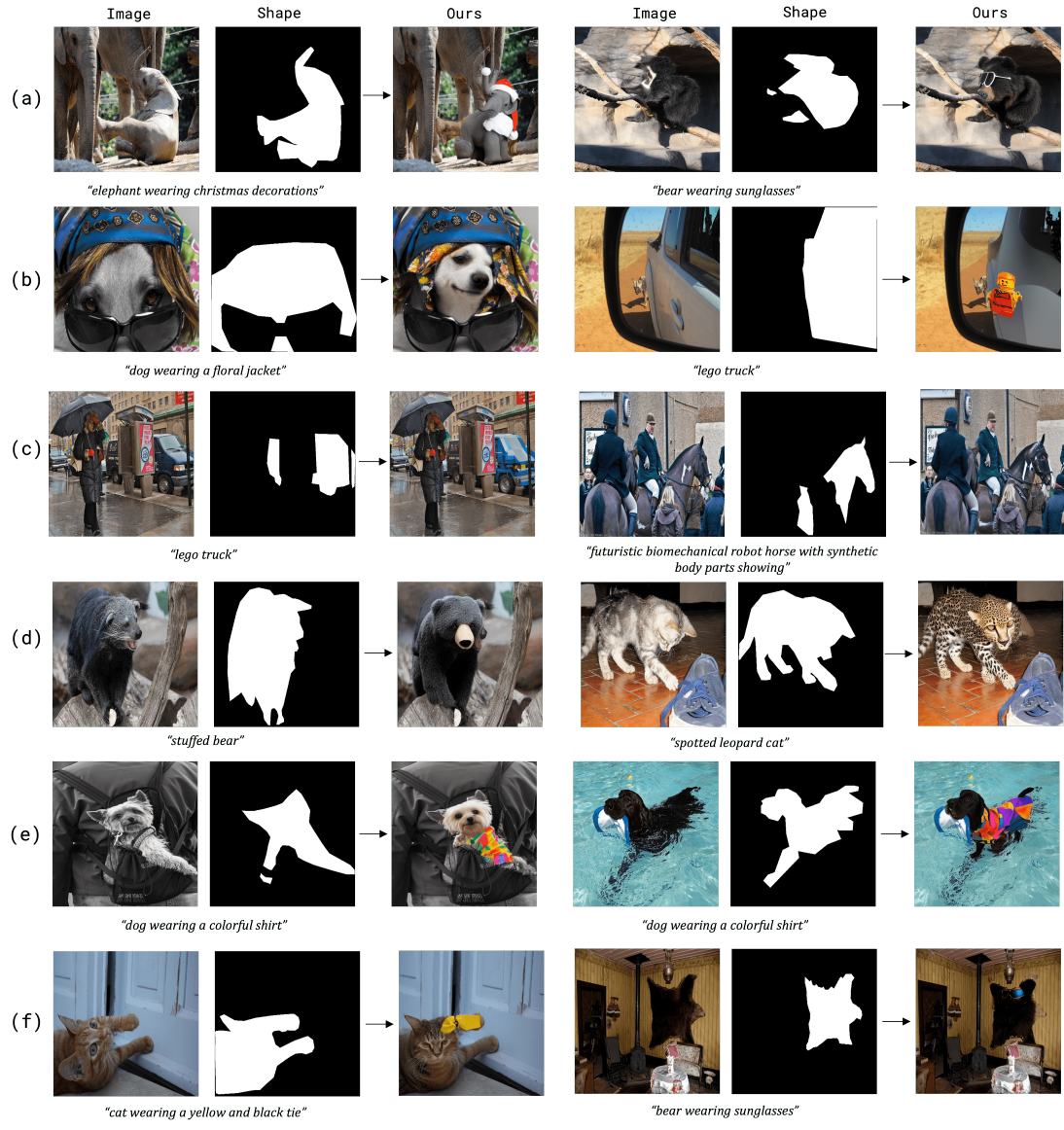


Figure 12. Examples of failure cases from our method that relate to (a) uncommon pose, (b) uncommon perspective, (c) multi-part mask, (d) ghosting, (e) global context, (f) accessory placement.

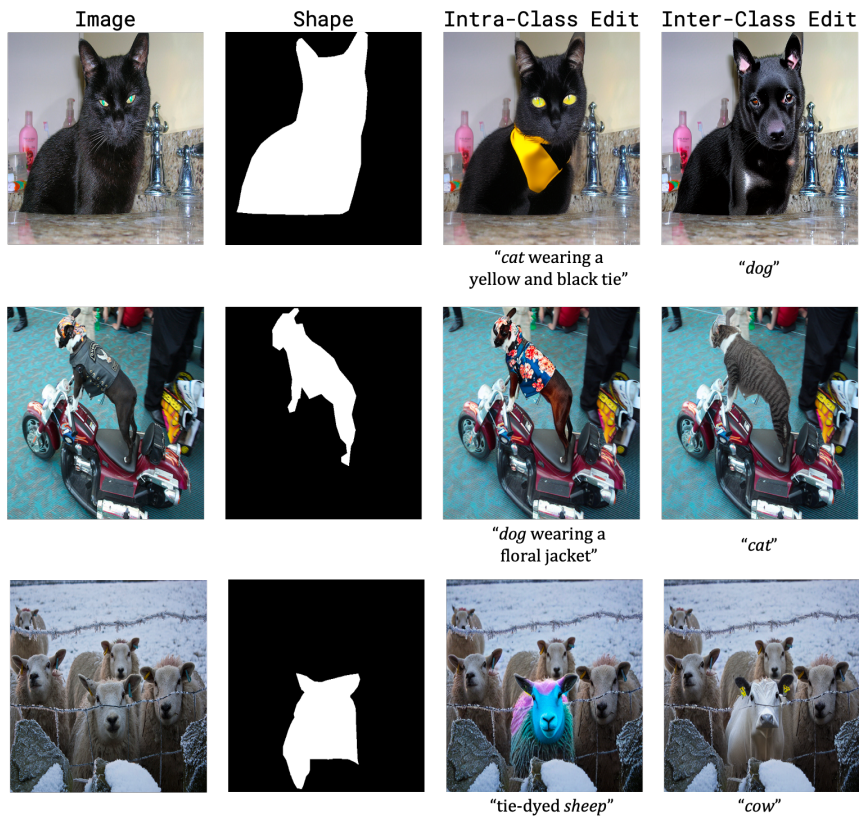


Figure 13. Additional examples of inter-class edits.

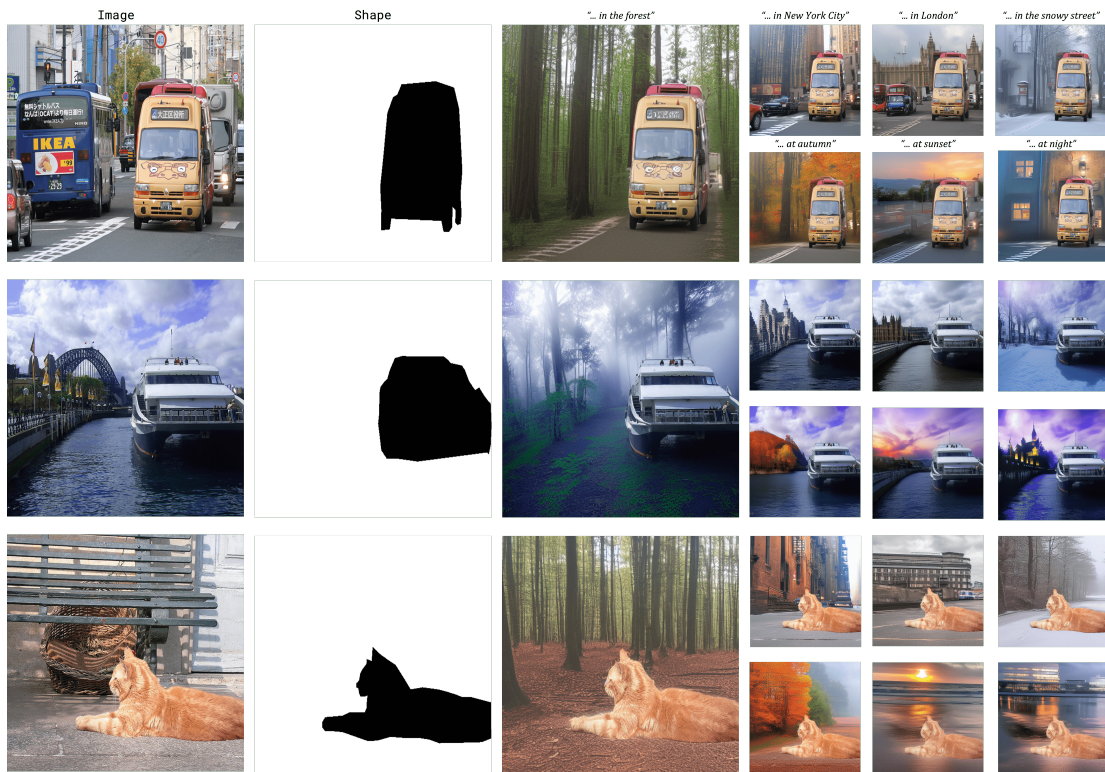


Figure 14. Examples of background edits from our method where we transform the background to various locations (New York City, London), seasons (winter, autumn), and times of day (sunset, night) for various objects (truck, boat, cat).

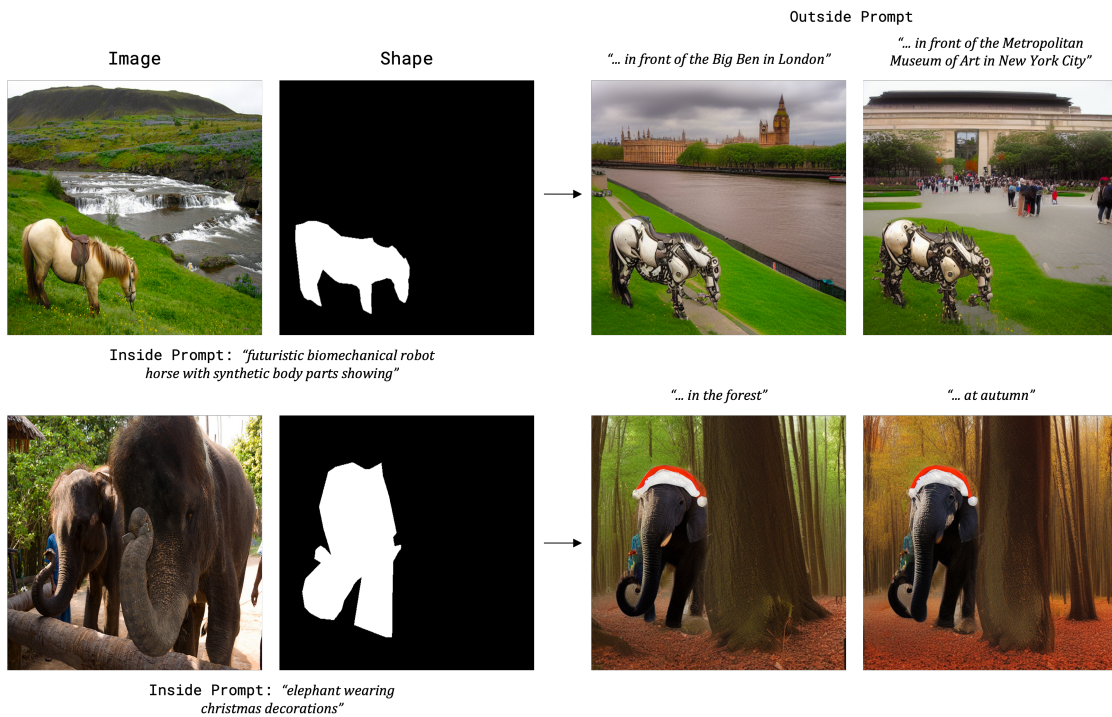


Figure 15. Examples of simultaneous inside and outside edits from our method. The inside and outside prompts used during inversion are object category names and “background”, respectively. The images are then edited by modifying both the inside and outside prompts. We show that our method is able to modify both the object within the mask and the background outside the mask according to their respective text prompts while maintaining the original shape of the object and the object’s relationship to the scene (i.e., horse grazing on grass, elephant occluded by another object).



Figure 16. Examples of our method applied with *automatically inferred* masks predicted by MaskFormer [3] including cases with (a) reflections, (b) multiple disjoint objects, (c) multiple overlapping objects, (d) imperfect masks, (e) standard clean masks.